In Vivo Evaluation of an Ultra-Fast Disintegrating Wafer Matrix: A Molecular Simulation Approach to the Ora-Mucoadhesivity

Deshika Reddy[1], Yahya E. Choonara[1], Pradeep Kumar[1], Mershen Govender[1], Sunaina Indermun[1], Lisa C. du Toit[1], Leith C.R. Meyer[2] and Viness Pillay[1]*

[1]Wits Advanced Drug Delivery Platform Research Unit, Department of Pharmacy and Pharmacology, School of Therapeutic Sciences, Faculty of Health Sciences, University of the Witwatersrand, Johannesburg, 7 York Road, Parktown, 2193, South Africa.

[2]University of Pretoria, Department of Paraclinical Sciences, Faculty of Veterinary Science, Pretoria, South Africa

***Corresponding Author:**
Professor Viness Pillay
Tel: +27-11-717-2274
Fax: +27-11-642-4355
Fax2Email: +27-86-553-4733
Email: viness.pillay@wits.ac.za

Graphical abstract

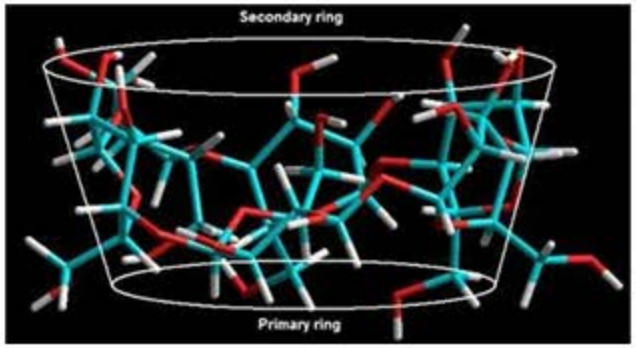

WAFER DELIVERY SYSTEM

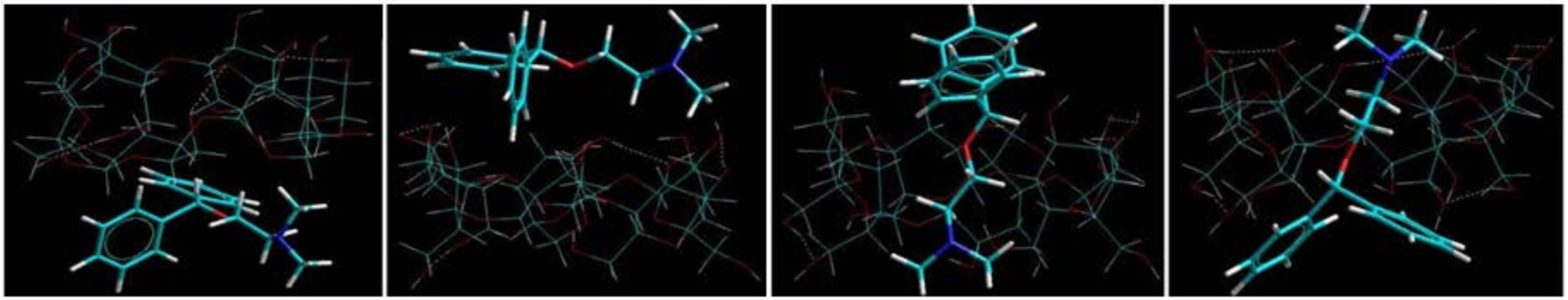

MOLECULAR ORIENTATION

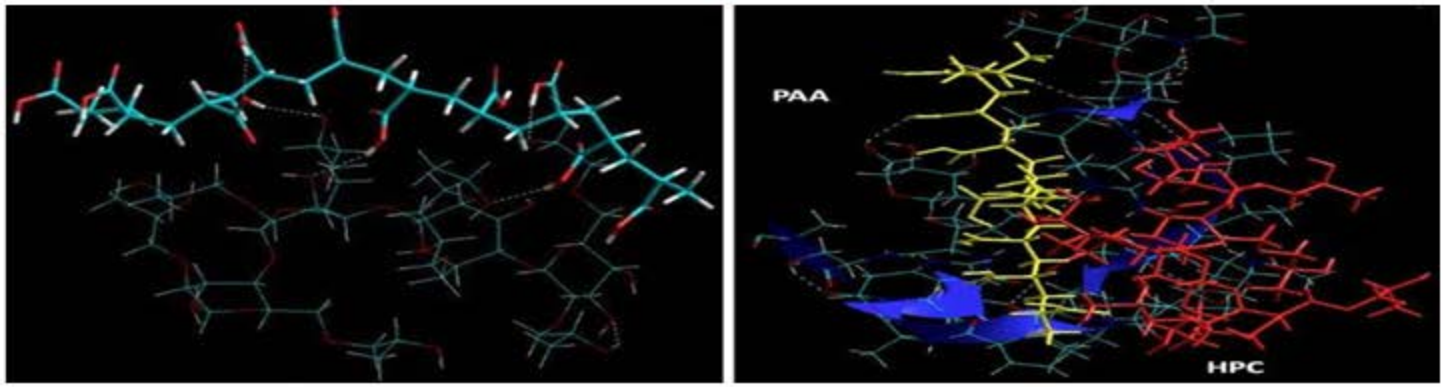

ORA-MUCOADHESION

Abstract

The purpose of this study was to design and evaluate the performance of an **Ultra-fast Disintegrating Wafer (U-D-WAF)** loaded with highly water soluble diphenhydramine hydrochloride (DPH) through the oramucosa of the Large White Pig model. In addition, for the first time this work explored the oramucosivity of the **U-D-WAF** by detailed molecular modeling of the matrix on buccal tissue in order to mechanistically deduce the mucodhesivity. The **U-D-WAF** was formulated using a blend of hydroxypropylcellulose, poly(acrylic) acid, sodium starch glycolate and β –cyclodextrin in accordance with a Box-Benkhen experimental design for optimization prior to *ex vivo* permeation and *in vivo release* studies in the Large White Pig. Molecular simulation studies assess the mucoadhesivity of the **U-D-WAF** to the oramucosa. A mean Drug Entrapment Efficiency of 72.96±4.32 %, disintegration time of 29.33±15.91 s and drug release after 60 s of 86.32±20.37 % was recorded. *Ex vivo* permeation studies revealed cumulative drug permeation of 86.32±20.34 % 60 s after onset. *In vivo* evaluation of the optimized **U-D-WAF** had a C_{max}=59 μgL^{-1} approximately 300 s after administration. The ultrafast disintegration of the **U-D-WAF** matrix with desirable mucoadhesivity in *in vitro* and *in vivo* studies makes it suitable for effective and rapid oramucosal drug delivery.

Keywords: Oramucosal drug delivery; wafer matrix; rapid disintegration; in vivo permeabilty; molecular modeling; mucoadhesivity

1. Introduction

The formulation of advanced rapidly disintegrating oramucosal drug delivery systems is lucrative due to the oral route being the most effective means of administering medication to patients[1-3]. A large degree of this route's success lies in its convenience and relative non-invasiveness, resulting in a high degree of patient compliance. Despite its advantages, conventional oral drug delivery is still subject to various shortcomings such as the loss of drug as a result of the hepatic 'first-pass' effect as well as the chemical degradation of sensitive pharmaceutical actives in the gastrointestinal tract[4,5]. The inability of certain patient groups (such as the physically and mentally disabled, pediatrics and geriatrics) to swallow a tablet or capsule also places additional constraints upon oral drug delivery[6,7].

In an attempt to circumvent a few of the disadvantages still associated with oral delivery systems, a variety of rapidly disintegrating drug delivery systems have been developed. These specialized formulations dissolve in the patient's mouth within a few seconds to minutes[2,8-11]. This provides the convenience of a tablet or capsule while simultaneously allowing for the ease of swallowing provided by a liquid formulation[12,13]. Generally, when this dosage form is placed in the mouth, contact with saliva causes it to disintegrate almost immediately into tiny particles, resulting in liberation of the drug molecules, which can thereafter be absorbed through the oramucosa. However, further exposure to saliva results in the particles dissolving into a drug-loaded suspension, which is then swallowed, exposing the drug to the gastric environment prior to conventional oral drug absorption and first-pass metabolism. Pre-gastric absorption therefore results in increased bioavailability of the drug since the potentially destructive gastric environment and hepatic metabolism is bypassed[14].

Wafer drug delivery is an advancing field which represents highly versatile polymeric devices consisting of porous matrices that allow for rapid delivery of drugs. Most wafers are produced via lyophilization, a process key to its rapidly disintegrating properties. The removal of unbound moisture from the wafer during the lyophilization process creates voids within the matrix resulting in the formation of a porous network which facilitates disintegration when exposed to the hydrophilic, saliva-rich oral cavity. In addition to being relatively cost-effective and simple to manufacture, wafers are also a highly efficient, versatile, and effective means of drug delivery. This is largely due to the ability of using wafers via the oral route to provide patients with quick, easy, and non-invasive pharmacological relief.

This study provides for the design, development and evaluation of an orally administered **Ultra-fast Disintegrating Wafer (U-D-WAF)** capable of delivering drug in an instantaneous

manner, through **the buccal mucosa**, into systemic circulation. Enhanced **U-D-WAF** disintegration was been achieved by using hydrophilic hydroxypropylcellulose (HPC) as one of the primary matrix-forming agents. HPC provides a physically robust matrix while still maintaining the desired rapid disintegration properties of the product[15]. HPC gels, either alone or in combination with other polymers, also avail varying degrees of bioadhesivity from which drugs have the potential to be constantly released. **β–cyclodextrin (β-CD) was used for taste-masking effects, whilst Sodium Starch Glycolate (SSG) was employed for its disintegrant properties**.The **U-D-WAF**, as part of this study, has been statistically optimized using an experimental design prior to extensive *in vitro* and *in vivo* characterization in the Large White pig model. In addition, for the first time this study explores the oramucosivity (mucoadhesivity to the oramucosa) employing detailed molecular modeling of the **U-D-WAF** matrix on buccal tissue to mechanistically ascertain the mucodhesive properties of the **U-D-WAF** after exposure to the oramucosa.

2. Materials and methods

2.1 Materials

Hydroxypropylcellulose (Klucel® EF, Brookfield Viscosity 150-700 cP 10 $\%^{w}/_{v}$ mucilage) was purchased from Hercules Inc. (North Carolina, USA). Poly(acrylic) acid (PAA), sodium starch glycolate (SSG, mean particle size 34 µm), diphenhydramine hydrochloride (DPH), β–cyclodextrin (β-CD) and methylparaben (MP) were purchased from Sigma Aldrich® (Kempton Park, Gauteng, South Africa). Lactose and mannitol were purchased from Merck Lab Supplies Pty. Ltd. (Midrand, Gauteng, South Africa). Glycine was purchased from Hopkin and Williams Pty. Ltd. (Essex, UK). All other reagents employed were of analytical grade and were used as received.

2.2 Experimental design

2.2.1 U-D-WAF preparation

Standard solutions of PAA (0.5-1.5 $\%^{w}/_{v}$) and HPC (4.0-6.0 $\%^{w}/_{v}$) were prepared and homogenously combined according to a randomized Box-Behnken statistical experimental design (Minitab® V15, Minitab Inc., PA, USA). **SSG (1.0–2.0$\%^{w}/_{v}$) and premixed DPH/β-CD complex (DPH: β-CD; 1:5 weight ratio) were thereafter added to the mixture under constant stirring.** The quantities of mannitol, lactose and glycine were kept constant in every formulation in accordance with Patel *et al*.[15]. The mixture was then homogenized for 15 **min** and left to stir for 24 h. The mixture was then cast into specially designed PVC molds, **having a diameter of 14 mm**, frozen at -70 °C for 24 h and thereafter lyophilized **(-**

64 °C; 1.5 mtorr) for a further 48 h. After lyophilization, the **U-D-WAFs** were extracted from the molds and stored at room temperature **(25°C)** in a desiccator until analysis. **Response optimization of the U-D-WAFs was subsequently carried out utilizing statistical software (Minitab1, V14, Minitab Inc1, PA, USA).**

2.2.1.1 Determination of the drug entrapment efficiency within the U-D-WAF

Drug Entrapment Efficiency (DEE) was calculated to determine the amount of drug contained in each batch of **U-D-WAF**. In order to calculate the DEE, the **U-D-WAFs** (***n***=5) were completely dissolved with continuous stirring in 20 mL of simulated saliva (SS; pH 6.75)[16]. The resulting solution was analyzed using UV spectroscopy at 254 nm. Drug content was assessed using Equation 1:

$$ggg\ (\%) = \frac{l\,l\,l\,l\,l\,l\,g\,g\,l\ g\ i\ i\ i\ l\ i\ i\ l\ g\,l\ l\,i\,i\,i}{Th\,i\ i\ g\,i\,l\,i\,l\,l\ l\ g\,g\,l\ g\ i\ i\ i\ l\ i\ i\ l\ g\,l\ l\,i\,i\,i} X\ 100 \quad \text{..... (1)}$$

2.2.2 Disintegration studies

Rapid disintegration studies were undertaken on the **U-D-WAF** formulations using the method as outlined by El-Arini et al.[17] with modifications. A Texture Analyzer (TA.XT*plus* Stable Microsystems, Surrey, UK) equipped with a flat, cylindrical probe **(20 mm diameter)**, was used to mimic the tongue's influence on the **U-D-WAF**. Individual wafers (***n***=3) were pre-weighed and the probe pre-wetted with **Simulated Saliva (SS)** onto which the **U-D-WAF** was affixed. The wetting of the probe provided sufficient moisture for the **U-D-WAF** face to undergo a minimal amount of gellation, thus requiring no other means of attachment. The sample was then lowered into a mini-petri dish (3.5 cm diameter) containing 1.5 mL SS (pH 6.75, 37±0.5 °C) at a predetermined force for 60 **s**. Disintegration was regarded to be complete when total loss of **U-D-WAF** structure was evident and the matrix had collapsed. The resultant distance-time profile was used to determine the onset of disintegration **(time at the onset of rapid increase of distance), disintegration rate (the first gradient of the descending region from the onset of disintegration before the point of inflection where disintegration rate decreased or stopped), and penetration distance of the probe through the wafer (initial distance prior to onset of disintegration).**

2.2.3 Physicomechanical integrity analysis

All physicomechanical integrity analysis studies (***n***=3) were conducted using the TA.XT*plus* Texture Analyzer fitted with a 5 kg load cell and a stainless steel needle-point probe. The testing parameters were configured such that the tip of the needlepoint probe passed completely through the center of the wafer matrix at a pre-determined force **(0.098N)**.

Graphs generated by the Texture Exponent 32® operating software were then analyzed to determine the physicomechanical properties of **U-D-WAF**. **All measured physicomechanical parameters ascertained were determined from the generated Force-Distance graphs and included the Energy of Absorption, Matrix Yield Value, Matrix Tolerance and the Matrix Resilience.**

2.2.4 Surface morphological studies

The surface morphology of **U-D-WAF** was determined using a FEI Phenom™ G2 Pro Desktop Scanning Electron Microscope (SEM) (Hillsboro, OR, USA). Each sample was mounted on aluminum stubs and sputter-coated with gold-palladium under a vacuum of 0.5 Torr (SPI-MODULE™ Control, SPI Supplies, PA, USA) prior to visualization.

2.2.5 Rheological analysis

Rotational rheometry was conducted on the gel-like residue that remained upon conclusion of disintegration testing, using a Haake Modular Advanced Rheometer System (ThermoFisher Scientific, Germany) at 37 °C. The profiles generated by the RheoWin® operating software were analyzed for shear stress, viscosity and deformation as a function of shear rate and time respectively. For analysis, the gel sample (***n***=3) was carefully loaded onto the rheometer plate in such a manner that shearing was minimal[18]. This gel sample was then hydrated with 1 mL of SS (pH 6.75, 37°C) and subjected to varying shear rates. The shear rate was ramped from 0.1-100 s^{-1} **[19]**. The average shear rate within the human oral cavity is reported to be between 0.1-1000 s^{-1}. Shear stress and deformation was measured as a function of the shear rate.

2.3 *Ex vivo* drug permeation analysis

Porcine buccal mucosa, obtained from a local abattoir (Mintko Meat Packers, Krugersdorp, Gauteng, South Africa), was used as a substitute for human oramucosal tissue for all *ex vivo* studies. All buccal tissue was excised in accordance with Good Laboratory Practice (GLP) standards and the methods outlined by Giannola et al.[20] before being flash frozen in liquid nitrogen and stored at -70 °C until use[20,21]. **The integrity of the porcine buccal mucosa was maintained during sourcing, storage and conduction of this analysis. This was done in accordance with the respective GLP protocols and standards.** All *ex vivo* release studies were conducted using a Franz Diffusion Apparatus, equipped with a 12mL receptor compartment. For this analysis, excised porcine buccal mucosa was sandwiched between the donor compartment, containing SS (pH 6.75) and the **U-D-WAF** to mimic the buccal cavity, and the receiver compartment containing simulated plasma (37 °C; pH 7.4)[22]

to mimic the systemic circulation. **The porcine mucosa was allowed to defrost to room temperature prior to analysis.** Samples **(1 mL)** from the receiver compartment were drawn after 20, 60, 180, 300, 600, 1800, 3600 and 5400 **s**, with an equal volume **(1 mL)** of simulated plasma (pH 7.4, 37±0.5°C) replaced after each sampling to maintain sink conditions. The concentration of drug in the receiver compartment was measured using UV spectroscopy.

2.4 *In vivo* studies in a Large White Pig model

Twelve healthy female Large White pigs (≈35kg) divided equally into 4 groups were used in the *in vivo* study. Group 1 was designated the control group **(administered with no formulation)** while groups 2 and 3 served to test the optimized **U-D-WAF** and the comparator product respectively. Group 4 was used as a placebo group in which **U-D-WAF** without drug was administered. All study groups were anaesthetized with midazolam (0.3 mg/kg I.M.) and ketamine (11 mg/kg I.M.). Isoflurane (2 %) in oxygen (100 %) was administered via a face mask to maintain anesthesia.

2.4.1 Dosing

A single optimized U-D-WAF was administered sublingually to the anesthetized pig to take advantage of natural pooling of saliva present in the area. The **U-D-WAF** was further wetted with 2 mL of SS that was syringed directly onto the system due to the anesthetics' tendency to dry secretions. **The U-D-WAF was administered sublingually tp prevent the premature removal of the U-D-WAF from the buccal mucosa by the pig over the test period. Blood samples were drawn at time points 0, 1, 3, 5, 10, 30, 45, and 60 min**. The pig was maintained under anesthesia throughout the duration of the study to ensure that accidental swallowing or chewing would not be a concern. Since there was no DPH-containing rapidly disintegrating oral drug delivery systems commercially available at the time of this study, capsules incorporating DPH were chosen as the comparator dosage product due to the systemic release of drug quicker than tablet. Blood samples were drawn at time points 0, 2, 4, 8, 16, 20 and 24 h. All collected blood samples were immediately stored in heparinized vacutainers and centrifuged (Nison Instrument (Shanghai) Limited, Shanghai, China) at a 15,000rpm for 15 **min**. The plasma supernatant was subsequently pipetted utilizing a micropipette (Boeco Gmbh, Hamburg, Germany) and stored at -70 ^{o}C until further use.

2.4.2 HPLC analysis

A Waters HPLC system (Waters Corporation, Milford, Massachusetts, USA) consisting of a Waters 1525 binary HPLC pump and a Waters 2489 UV/Visible detector was used for

sample analysis. The chromatographic separation was performed on a C18 column (100mm x 3.0 mm, 3.5 µm particle size) at a column temperature of 30ºC **and a wavelength of 254 nm.** The mobile phase was composed of water/acetonitrile/formic acid (65:35:0.1) operated at a flow rate of 1 mL/min[23]. The injection volume was 20 µL and the analysis time was 8 **min** per sample.

2.4.2.1 Drug extraction

Plasma samples stored at -70 ºC were left to equilibrate at room temperature. To a 600 µL aliquot of plasma, 50µL of MP standard solution (1 µg/mL) and 600 µL of 0.6 M NaOH were added, horizontally shaken and centrifuged at 2500 rpm for 5 **min** to mix. The centrifuged sample was then extracted with 3 mL of *n*-hexane:diethylether (80:20). The supernatant was syringed out and concentrated to dryness under a stream of nitrogen gas at room 30ºC and subsequently reconstituted with 1 mL DMSO prior to analysis[24,25].

2.5 Atomistic molecular structural mechanics simulations

In order to obtain an overall understanding of the underlying mechanisms governing the physicochemical and physicomechanical attributes of the **U-D-WAF in addition to understanding the mucoadhesive potential of the U-D-WAF thereby ensuring optimal drug delivery**, Molecular Mechanics Computations in vacuum, which included the model building of the energy-minimized structures of drug–β-CD, and polymer-mucopeptide complexes, were performed using the HyperChem™ 8.0.8 Molecular Modeling System (Hypercube Inc., Gainesville, Florida, USA) and ChemBio3D Ultra 11.0 (CambridgeSoft Corporation, Cambridge, UK)[26]. Sugars, HPC and β-CD, were constructed in a chair conformation by the use of standard bond lengths and bond angles using sugar builder module on HyperChem 8.0.8. β-CD was modelled by the incorporation into a macrocyclic ring of six o-glucose projections where each torsional angle at α (1-4) glycosidic linkage between the rings gave a regular torus structure of 6-fold symmetry. The structure diphenhydramine (DPH) were built up with natural bond angles as defined in the Hyperchem software. The PAA decamer was drawn using ChemBio3D Ultra in its syndiotactic stereochemistry as a 3D model. **The structure of the glycosylated oromucopeptide analogue (MUC; glycosylated Pro-Asp-Thr-Arg sequence) was generated using the sequence editor module on HyperChem 8.0.8.** The generation of the overall steric energy associated with the energy-minimized structures was initially executed initially via energy-minimization using MM+ force field and the resulting structures were again energy-minimized using the Amber 3 (Assisted Model Building and Energy Refinements) force field. The conformer having the lowest energy was used to create the DPH-β-CD and HPC-PAA complexes.

Two different approaches, lateral alignment and insertion, were adopted for the relative arrangements of DPH and β-CD. In former case, the molecule was further allowed to approach the β-CD cavity laterally from two lateral orientations: the narrower rim which contains the primary hydroxyl groups (β-CD-DPH_1) and other from the secondary hydroxyl rim (β-CD-DPH_2) (Fig. 1). In case of insertion model, the complexation arrangement was obtained by the manual insertion of DPH in vertical position into the β-CD cavity, through the primary (β-CD-DPH_3) and secondary hydroxyl group rim (β-CD-DPH_4) and perpendicularly to its diameter via the phenyl ring end. HPC, PAA and MUC were modelled to generate: HPC/PAA and HPC/PAA/MUC. Full geometry optimizations were carried out in vacuum employing the Polak–Ribiere conjugate gradient method with several algorithms (at first, steepest descent, followed by conjugate gradient to refine the structure) until an RMS gradient of 0.001kcal/mol was reached. Force field options in the AMBER (with all hydrogen atoms explicitly included) and MM+ (extended to incorporate non-bonded cut-offs and restraints) methods were the HyperChem 8.0.8 defaults. For calculations of energy attributes, the force fields were utilized with a distance-dependent dielectric constant scaled by a factor of 1. The 1-4 scale factors are following: electrostatic 0.5 and van der Waals 0.5.

3. RESULTS AND DISCUSSION

3.1 Assessment of U-D-WAF Drug Entrapment Efficiency and disintegration

Average Drug Entrapment Efficiency (DEE) of the 15 Box-Behnken design formulations was calculated at 72.96 % (SD±45.53). Formulations containing a greater than 4 $\%^{w}/_{v}$ HPC concentration were determined to have a greater degree of drug entrapment. This can be attributed to the relatively viscous nature of the polymer solution facilitating better drug retention within the **U-D-WAF** matrix. Being an intrinsically hydrophilic molecule, DPH is better entrapped within this relatively highly entangled polymeric network as compared to less concentrated solutions. The large standard deviations depicted can also be attributed to the effects mediated via polymer concentrations in the **U-D-WAF** matrix.

Disintegration profiling of the respective experimental design formulations revealed extended onsets of disintegration despite possessing relatively good disintegration rates and times (Table 1). The variation in disintegration rate was noted to be largely dependent on the concentrations of polymers and SSG used. This can be considered as a characteristic behavior of the highly hydrophilic core components within the **U-D-WAF** that were exploited

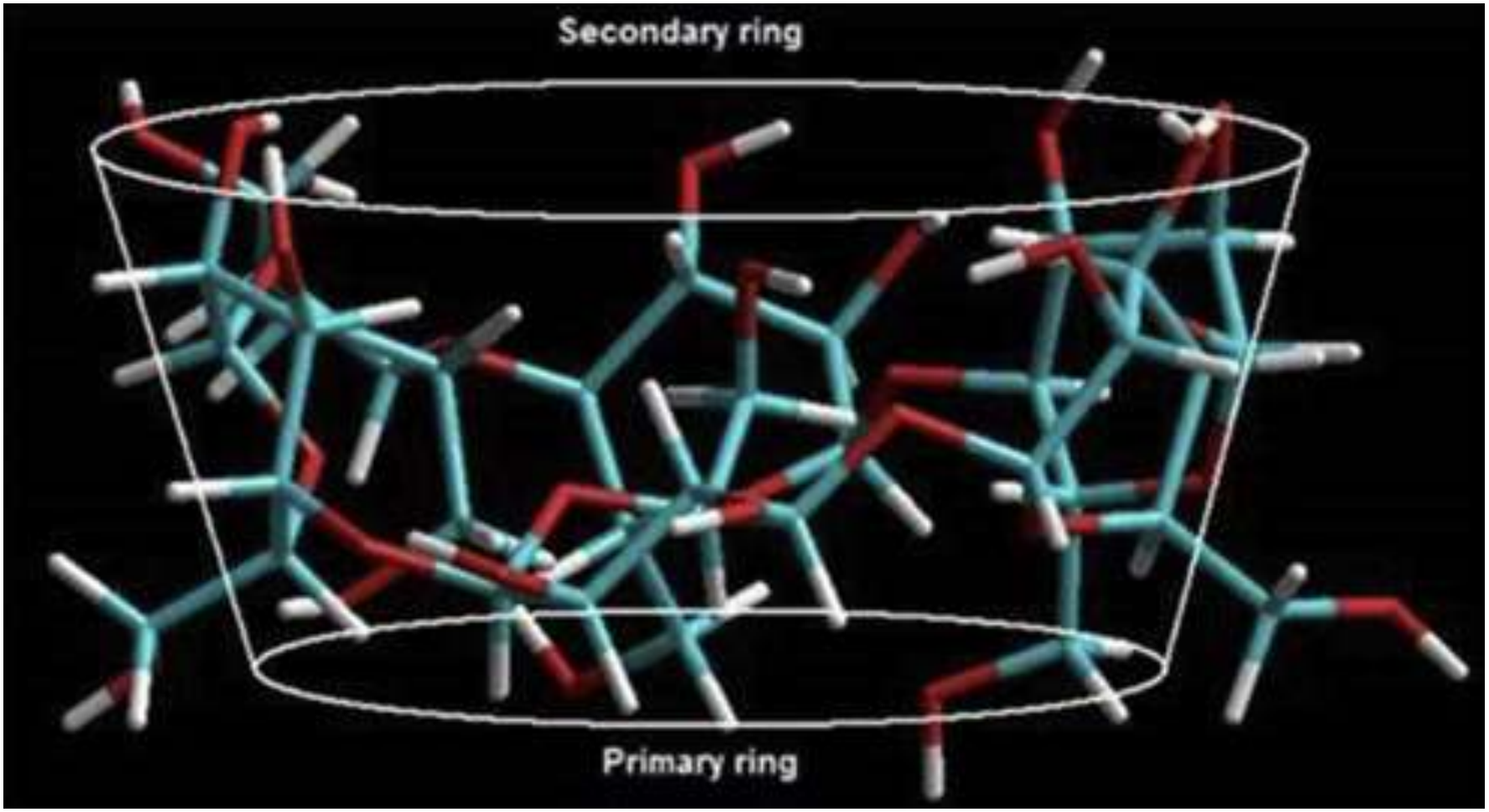

Fig. 1. Stereographic view of β-cyclodextrin bucket showing primary and secondary rim.

Table 1. Observed WDS disintegration in the Box-Behnken Design

Formulation Number	WDS Matrix Constituent (%$^{w}/_{v}$)			Parameter	
	HPC	PAA	SSG	ADT (sec)	±SD
1	4.0	1.5	1.5	16.61	**10.70**
2	6.0	1.0	2.0	60.00	**19.98**
3	4.0	1.0	2.0	16.94	**10.47**
4	5.0	1.0	1.5	18.23	**9.56**
5	5.0	1.5	1.0	26.69	**3.57**
6	6.0	1.5	1.5	43.56	**8.36**
7	4.0	1.0	1.0	28.24	**2.48**
8	5.0	1.0	1.5	18.64	**9.26**
9	5.0	0.5	1.0	25.82	**4.19**
10	6.0	0.5	1.5	31.53	**0.15**
11	5.0	0.5	2.0	60.00	**19.31**
12	5.0	1.0	1.5	23.10	**6.11**
12	5.0	1.5	2.0	14.83	**11.95**
14	4.0	0.5	1.5	60.00	**18.85**
15	6.0	1.0	1.0	31.91	**0.12**

HPC: Hydroxypropylcellulose; PAA: Poly(acrylic) acid; SSG: Sodium starch glycolate; ADT: Average disintegration time; SD: Standard deviation

to facilitate rapid **U-D-WAF** disintegration and subsequent drug release. Disintegration times ranged from 16.61 to 60 **s** with an average of 29.33 **s**. **U-D-WAFs** containing lower concentrations of HPC and PAA were determined to produce superior disintegration profiles when compared to formulations possessing higher concentrations of these polymers. Specifically, formulations 1 and 3 containing 4 $\%^{w}/_{v}$ HPC displayed an average disintegration times of below 17.00 **s**.

Despite being invaluable to the overall disintegration of **U-D-WAF** matrix, SSG did not exert itself on a significant level in those formulations containing higher concentrations of HPC and PAA, with disintegration times of these formulations exceeding 60 **s** (Formulations 2, 12 and 14). This phenomenon was more clearly perceived in those formulations containing 6 $\%^{w}/_{v}$ HPC rather than those with a high concentration of PAA. These relatively viscous formulations resulted in a greater degree of polymeric chain overlap, or tangling, in which water soluble SSG particles were trapped[27]. As a result of this, SSG presents a decreased surface area for wetting, thus impeding its ability to swell in a hydrophilic medium to exert its superdisintegrant properties. Consequently, the relatively time consuming procedure of fluid infiltration into the matrix and disentangling of HPC chains must first occur before SSG is seen to have a tangible effect upon **U-D-WAF** disintegration. Control formulations containing similar polymer constituents without SSG displayed incomplete disintegration after 60 **s**, generally taking 10 **min** in excess to accomplish a comparable level of disintegration as experimental design run formulations containing stipulated SSG quantities. This control therefore validates the use of SSG in the **U-D-WAF** formulation.

3.2 Evaluation of the physicomechanical integrity of the U-D-WAF matrix

U-D-WAF formulations with the highest matrix energy absorption values were those that consisted of a 6 $\%^{w}/_{v}$ HPC solution (Formulations 6 and 15), with an average value of 8.869 N.mm (SD±1.23), significantly higher than the total average matrix energy absorption value of 4.48 N.mm (SD±0.47) of all the formulations evaluated (Table 2). **The matrix energy absorption was measured by determining the Area Under the Curve (AUC) of the Force-Distance profile and is an indirect determinant of porosity of a sample.** Despite the relatively high energy of absorption value, the majority of 6 $\%^{w}/_{v}$ HPC formulations were extremely brittle and difficult to extract from moulds. A high degree of breakage occurred, with these **U-D-WAFs** being highly prone to flaking which implies relatively low matrix tolerance values despite the bulking provided by the relatively high HPC concentration.

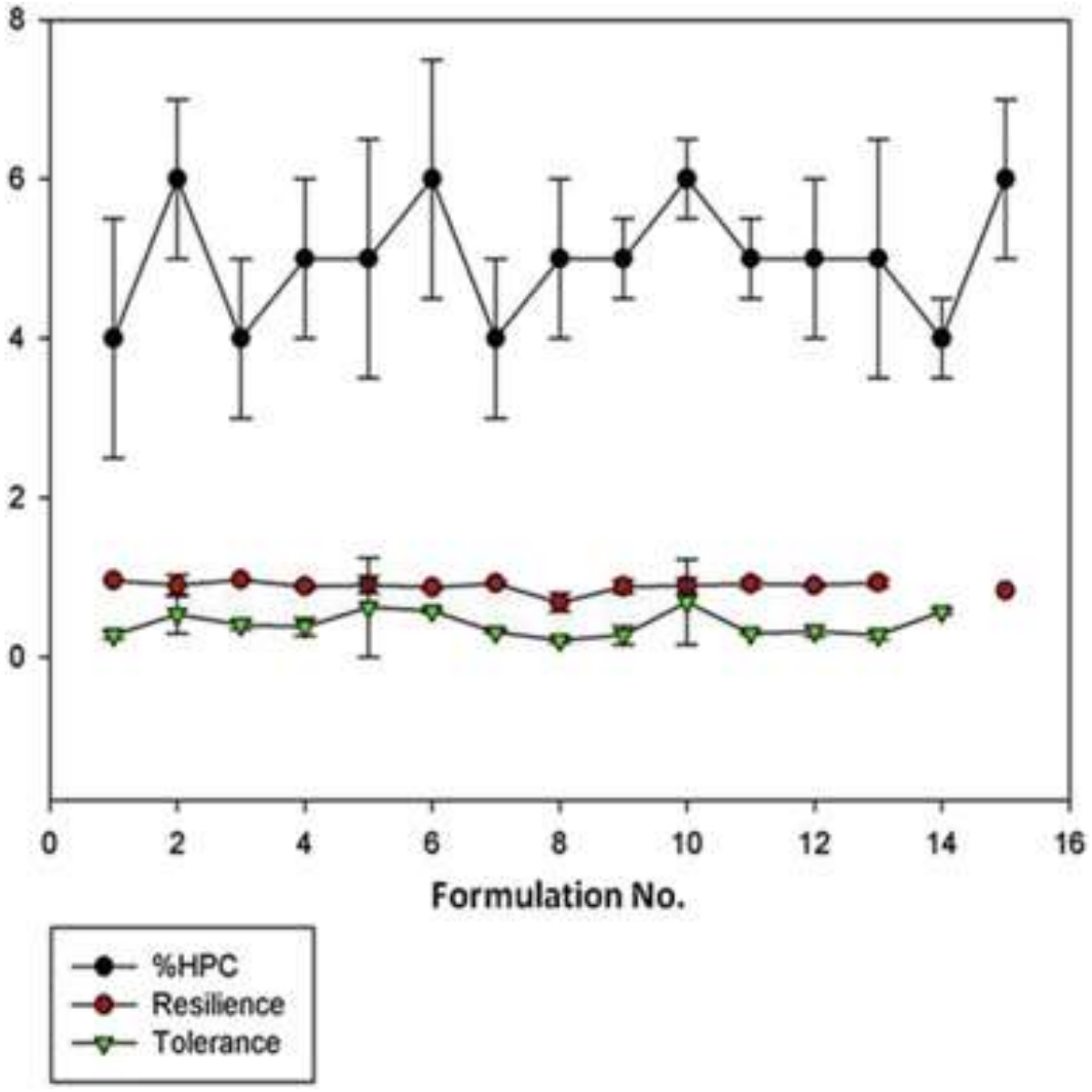

Fig. 2. Profile depicting the relationship between HPC concentrations and matrix resilience and tolerance of respective U-D-WAF formulations (SD < 0.25 in all cases).

Table 2. Average matrix tolerance, resilience and energy of absorbance values of the Box-Behnken design formulation

Formulation	Average Tolerance (Nm^{-1})	±SD	Average Resilience ($N.mm^{-1}$)	±SD	Average Energy of Absorption (N.mm)	±SD
1	**0.28**	**0.04**	**0.96**	**0.00**	**3.93**	**0.58**
2	**0.53**	**0.25**	**0.90**	**0.13**	**1.95**	**1.00**
3	**0.41**	**0.06**	**0.98**	**0.00**	**5.16**	**0.47**
4	**0.38**	**0.11**	**0.86**	**0.04**	**5.00**	**0.75**
5	**0.62**	**0.62**	**0.91**	**0.11**	**0.58**	**0.51**
6	**0.58**	**0.03**	**0.87**	**0.02**	**9.32**	**1.18**
7	**0.31**	**0.02**	**0.92**	**0.02**	**5.13**	**0.47**
8	**0.21**	**0.04**	**0.68**	**0.12**	**1.66**	**0.81**
9	**0.27**	**0.12**	**0.89**	**0.08**	**2.78**	**0.37**
10	**0.69**	**0.53**	**0.89**	**0.09**	**4.53**	**2.15**
11	**0.29**	**0.01**	**0.92**	**0.06**	**4.49**	**0.29**
12	**0.32**	**0.06**	**0.90**	**0.03**	**5.14**	**0.42**
13	**0.28**	**0.06**	**0.94**	**0.06**	**4.66**	**0.84**
14	**CNBD**	**CNBD**	**CNBD**	**CNBD**	**CNBD**	**CNBD**
15	**0.57**	**0.03**	**0.83**	**0.07**	**8.42**	**1.28**

SD: Standard deviation; CNBD: Could not be determined

Matrix integrity was vastly improved in formulations that had high concentrations of HPC, PAA and SSG due to the bulking effect found within the **U-D-WAF** matrix. Fig. 2 depicts this relationship between **U-D-WAF** HPC concentrations and **U-D-WAF** tolerance and resilience. Paradoxically, the 4 $\%^{w}/_{v}$ HPC **U-D-WAF** formulations displayed higher matrix energy absorption values than their 5 $\%^{w}/_{v}$ equivalents. In addition to this, these formulations also displayed some level of matrix robustness, with best overall matrix yield value with an average value of 1.75 Nmm^{-1} (SD±0.25). The overall average matrix yield totaled 1.18 Nm^{-1} (SD±0.18). **U-D-WAFs** also proved to be highly resilient, with an average resilience of **0.89 $N.mm^{-1}$** (SD±0.07) as illustrated in Table 2. This contradicts the traditional image of lyophilized products being structurally unsound and ill-equipped to deal with the rigors of packaging and handling[28]. The average matrix tolerance, resilience and energy of absorbance for Formulation 14 could not be determined due to the properties of the **U-D-WAF** matrix produced.

3.3 Surface morphology of the U-D-WAF matrices

Scanning electron microscopy images of the respective experimental design formulations noted significant differences in surface morphology, dependent largely on the quantity of the polymeric constituents used. Fig. 3a, which depicts a **U-D-WAF** formulation with a greater quantity of polymeric constituents, was seen to have decreased surface porosity when compared to the **U-D-WAF** matrices containing low to medium quantities of polymer solution. This property is in correlation with the longer disintegration times determined whereby a decreased surface porosity inhibited matrix hydration. Fig. 3b, which depicts a **U-D-WAF** formulation with a lower quantity of polymeric constituents, in contrast has significantly larger surface pores and therefore hydrates far more quickly. This therefore results in the lower disintegration time seen previously.

3.4 Response optimization of the U-D-WAF

Determination of the optimal levels of each respective independent variables was conducted utilizing Minitab® V15 statistical software. The formulation was optimized for the measured responses of average disintegration time, drug release and permeation and DEE, such that concentrations of HPC, PAA and SSG were obtained for the production of a rapidly disintegrating U-D-WAF. Statistical optimization of the

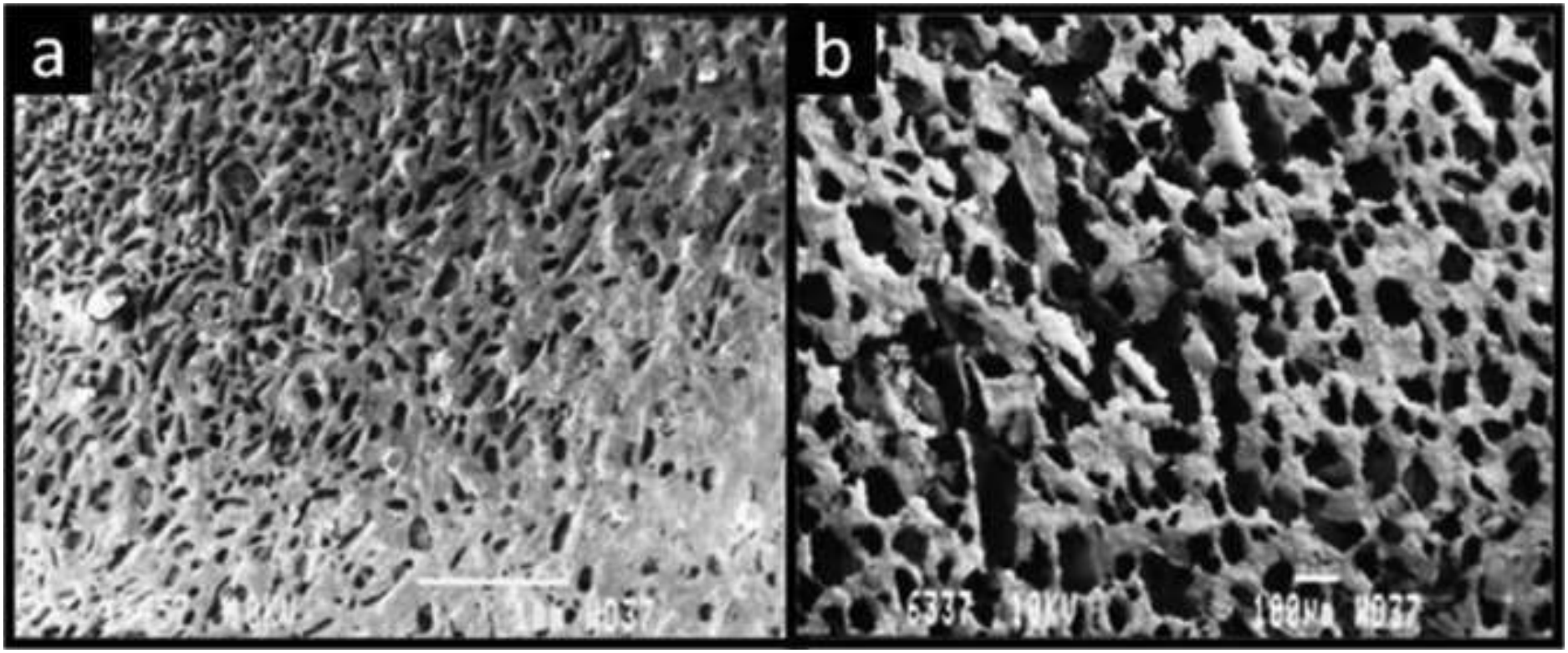

Fig. 3. SEM images of experimental design formulations exhibiting: (a) a less porous matrix resulting from concentrated constituent polymer solution and (b) a porous matrix resulting from less concentrated constituent polymer solution (Magnification = 100x).

U-D-WAF yielded an ideal matrix consisting of polymeric concentrations of HPC, PAA and SSG of 4.0, 1.5 and 1.6 (% w/v), respectively.

3.5 Rheological assessment of the gel residue component of the U-D-WAF

The gel remaining upon the completion of disintegration is an artifact of the gelling of PAA, HPC and SSG. After disintegration, this gel must adhere onto the oramucosa and withstand the relatively high shear processes of salivary flow, tongue movement, temperature fluctuations, chewing, swallowing and talking without being dislodged. Since these processes occur in mouth normally, their influence upon the characteristics of the gel was investigated and related to its ability to adhere to the oramucosa. The maximum shear stress required to deform the residue ranged between 180-1717 τ, at an average of 705.85 τ (***n***=45, SD±492.6). Polymer concentration was once more observed to impact the viscosity and subsequent shear needed within the oral cavity to dissolve the gel and systemically release agglomerated drug. Formulations with higher concentrations of **U-D-WAF** matrix constituents were seen to require a greater amount of shear in order to adequately disperse the gel. It was inferred from this that shear rate is indicative of the overall **mucoadhesivity** of the gel[29]. The degree of **mucoadhesivity** appeared to decrease with increasing concentrations of SSG. Conversely however, **mucoadhesivity** increased correspondingly with increasing concentrations of the PAA, whilst increased concentrations of HPC served to merely increase the viscosity of the gel as illustrated in Fig. 4. The viscous nature of this gel coupled with its ability to withstand a relatively high shear rate further demonstrates its ability to remain undisturbed in the oral cavity, ultimately allowing for constant release of drug.

3.6 *Ex vivo* drug permeation studies

Average cumulative drug permeation of the 15 batches of experimental design **U-D-WAFs** was determined to be 86.32 % (***n***=45, SD±20.34) at 60 **s** (Fig. 5). Formulations containing lower concentrations of HPC and higher concentrations of SSG were seen to produce almost complete drug permeation within the first minute of testing. The swiftness and completeness of drug release and permeation in such formulations can be attributed to the formulation's rapidly disintegrating nature. When exposed to SS (pH 6.75, 37±0.5°C), the polymeric chains comprising the low viscosity HPC backbone proceed to disentangle in a degree that is proportional to fluid infiltration within the matrix. In addition, SSG is simultaneously wetted with SS, causing it to swell and further contributed towards matrix collapse. Formulations containing relatively higher concentrations of SSG were thus able to

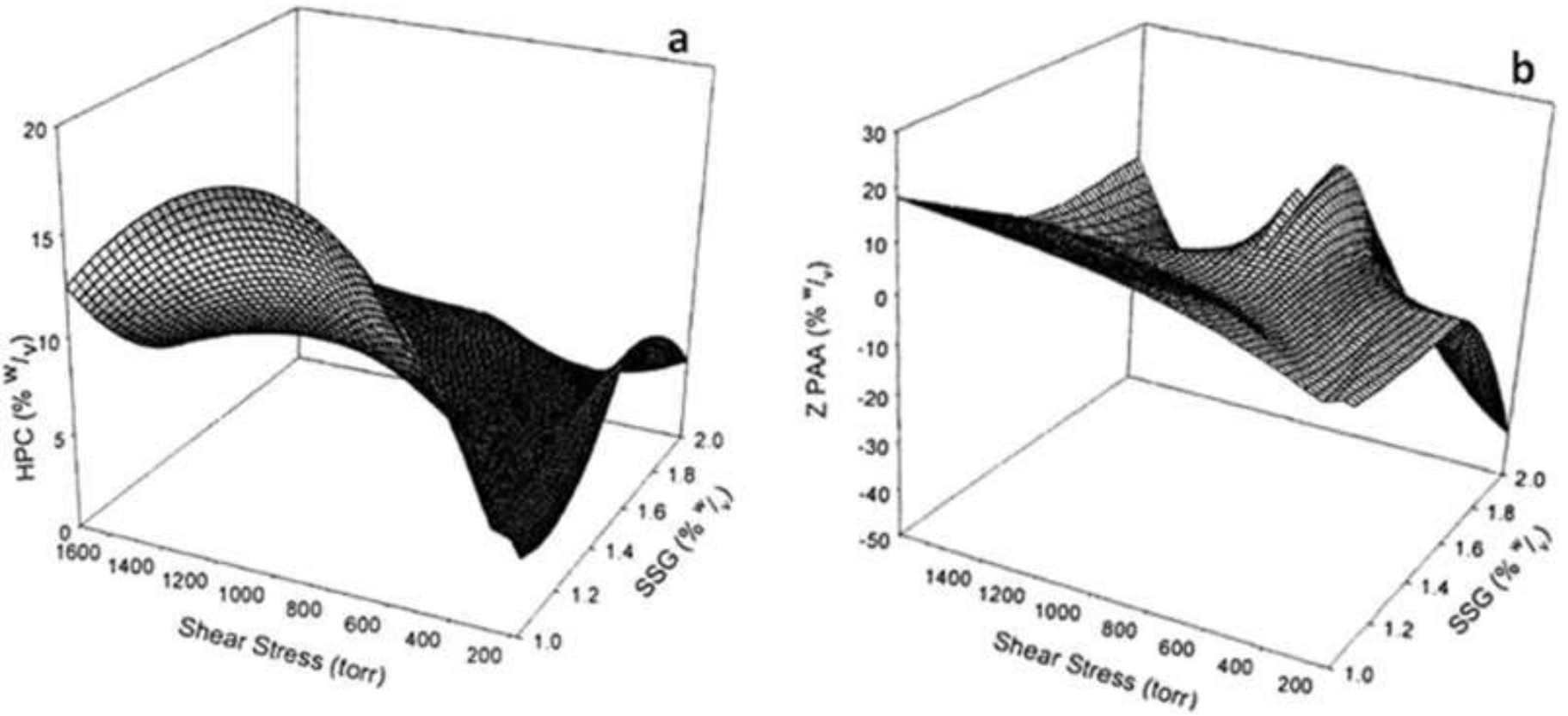

Fig. 4. Surface plots depicting the effect of (a) HPC and SSG and (b) PAA and SSG concentrations on gel viscosity and shear stress.

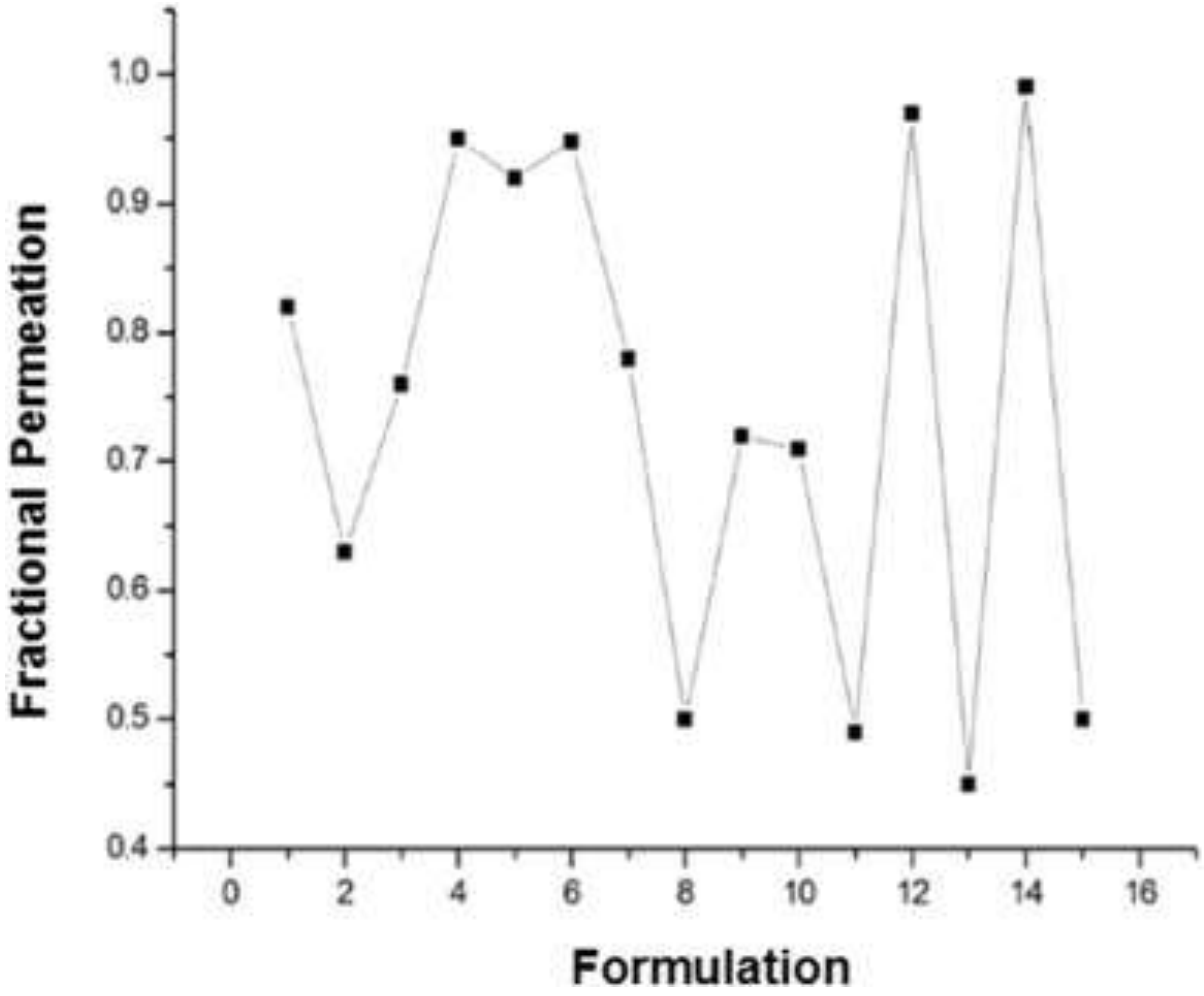

Fig. 5. Fractional drug permeation of the U-D-WAF design formulations within the first 60 s of testing (n = 15, SD < 0.40 in all cases).

more comprehensively assist with matrix disintegration; hence these **U-D-WAFs** displayed a higher fractional drug release and permeation. PAA's contact with SS results in its swelling to form a hydrated matrix layer in the form of a gel[30]. Instead of entangled polymer chains, PAA forms discrete microgels composed of polymer particles in which the drug is dispersed. Higher PAA concentrations appear to negatively impact the amount of drug able to be liberated from the **U-D-WAF** matrix for absorption over the time constraints required for rapid drug release; the viscosity of the microgels produced parallels that of PAA concentrations. Thus, the more concentrated PAA is, the more viscous the microgel, implying less drug is able to be readily released for systemic absorption. This formulation is, however, capable of releasing embedded drug constantly over an extended time period of approximately 15 **min** as displayed in the experimental design formulations tested.

3.7 *In vivo* releaseanalysis

The drug release and permeation results for the optimized **U-D-WAF** demonstrated a spike in drug concentration (C_{max} = 59 μgL^{-1}) at approximately 300 **s** (Fig. 6), high than the *ex vivo* permeation results that exhibited peak concentrations after 60 **s**. This disparity can be justified by the anticholinergic side-effects of the sedatives and general anesthetics that were administered to the animals prior to the study which serves to dry secretions, including saliva. This resulted in a reduced degree of wetting of the **U-D-WAF** which negatively impacted its disintegration and dissolution rates *in vivo.* The *in vivo* drug release profile for the comparator exhibited a C_{max}=48.15 μgL^{-1} attained at a T_{max}=75 **min** (Figure 6). The relatively sedate rate of drug release can be attributed to the relatively lengthy dissolution process undergone by the capsule which contrasts that of the optimized **U-D-WAF**. The gelatin shell of the capsule needs to be sufficiently wetted for swelling and subsequent rupture to occur. Further fluid infiltration must then occur before the contents of the capsule is liberated for systemic absorption to occur. **The AUCs of the U-D-WAF and the comparator product was calculated to be 1020.75 and 3592.5, respectively. The large difference can be attributed to the dose of the U-D-WAF (4.5mg) when compared to the comparator product (50mg).** Based on the study its conclusive that optimized rapidly disintegrating oramucosal **U-D-WAF** is able to achieve a greater degree of systemic drug release in a shorter period of time than its comparator product.

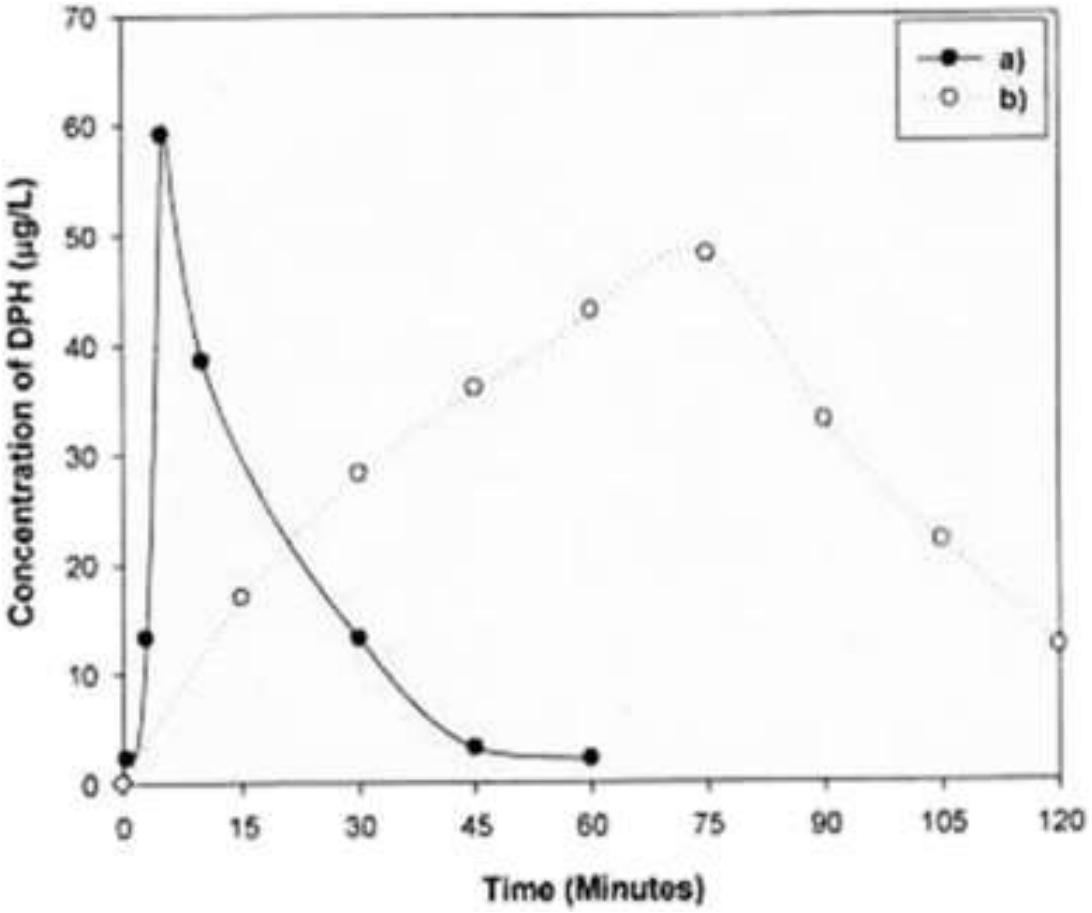

Fig. 6. Pharmacokinetic profile of DPH in plasma of a) the optimized U-D-WAF and b) the comparative capsule formulation.

3.8 Molecular mechanics assisted model building and energy refinements

A molecular mechanics conformational searching procedure was employed to acquire the data employed in the statistical mechanics analysis, and to obtain differential binding energies of a Polak–Ribiere algorithm and to potentially permit application to drug-cyclodextrin and polymer-protein assemblies. MM+ is a HyperChem modification and extension of Norman Allinger's Molecular Mechanics program MM2[31] whereas AMBER, is a package of computer programs for applying molecular mechanics, normal mode analysis, molecular dynamics and free energy calculations to simulate the structural and energetic properties of molecules[32].

3.8.1 Molecular mechanics energy relationship analysis

Molecular mechanics energy relationship (MMER), a method for analytico-mathematical representation of potential energy surfaces, was used to provide information about the contributions of valence terms, non-covalent Coulombic terms, and non-covalent van der Waals interactions for the DPH-β-CD morphologies and the HPC-PAA/MUC composites. The MMER model for the potential/steric energy factors in various molecular complexes can be written as:

$\mathbf{E_{molecule/complex}} = V_\Sigma = V_b + V_\theta + V_\varphi + V_{ij} + V_{hb} + V_{el}$ ...(2)

$\mathbf{E_{\beta\text{-}CD}} = 5.632V_\Sigma = 4.639V_b + 35.558V_\theta + 69.555V_\varphi + 21.314V_{ij} - 3.661V_{hb} - 121.774V_{el}$ ...(3)

$\mathbf{E_{DPH}} = 8.848V_\Sigma = 0.560V_b + 1.230V_\theta + 0.379V_\varphi + 6.677V_{ij}$ ...(4)

$\mathbf{E_{\beta\text{-}CD\text{-}DPH1}} = -10.581V_\Sigma = 5.067V_b + 36.823V_\theta + 73.693V_\varphi + 16.156V_{ij} - 4.993V_{hb} - 137.328V_{el}$ ...(5)

ΔE = -25.061kcal/mol

$\mathbf{E_{\beta\text{-}CD\text{-}DPH2}} = -12.784V_\Sigma = 4.967V_b + 38.059V_\theta + 68.231V_\varphi + 8.710V_{ij} - 4.221V_{hb} - 128.532V_{el}$ ...(6)

ΔE = -27.264kcal/mol

$\mathbf{E_{\beta\text{-}CD\text{-}DPH3}} = -26.021V_\Sigma = 5.134V_b + 35.670V_\theta + 68.667V_\varphi + 14.231V_{ij} - 3.342V_{hb} - 146.384V_{el}$ ...(7)

ΔE = -40.501kcal/mol

$\mathbf{E_{\beta\text{-}CD\text{-}DPH4}} = -17.197V_\Sigma = 5.033V_b + 37.259V_\theta + 66.393V_\varphi + 10.585V_{ij} - 3.492V_{hb} - 132.977V_{el}$ ...(8)

ΔE = -31.677kcal/mol

$\mathbf{E_{HPC}} = 62.520V_\Sigma = 3.656V_b + 29.523V_\theta + 43.723V_\varphi + 9.136V_{ij} - 1.605V_{hb} - 21.914V_{el}$ ...(9)

$\mathbf{E_{PAA}} = 10.257V_\Sigma = 1.517V_b + 7.178V_\theta + 4.244V_\varphi - 2.540V_{ij} - 0.141V_{hb}$ ...(10)

$\mathbf{E_{HPC/PAA}} = 29.117V_\Sigma = 4.975V_b + 35.721V_\theta + 48.381V_\varphi - 15.283V_{ij} - 0.897V_{hb} - 43.780V_{el}$ ...(11)

ΔE = -43.660kcal/mol

$\mathbf{E_{MUC}} = -166.812V_\Sigma = 5.474V_b + 70.351V_\theta + 55.173V_\varphi - 29.066V_{ij} - 7.096V_{hb} - 261.649V_{el}$ ...(12)

$\mathbf{E_{HPC/PAA/MUC}} = -183.135V_\Sigma = 10.932V_b + 115.859V_\theta + 102.949V_\varphi - 72.098V_{ij} - 8.450V_{hb} - 332.327V_{el}$ ...(13) **ΔE = -89.100kcal/mol**

where, V_{Σ} is related to total steric energy for an optimized structure, V_b corresponds to bond stretching contributions (reference values were assigned to all of a structure's bond lengths), V_{θ} denotes bond angle contributions (reference values were assigned to all of a structure's bond angles), V_{φ} represents torsional contribution arising from deviations from optimum dihedral angles, V_{ij} incorporates van der Waals interactions due to non-bonded interatomic distances, V_{hb} symbolizes hydrogen-bond energy function and V_{el} stands for electrostatic energy.

3.8.2 DPH-β-CD molecular mechanics simulations at different orientations

The energy minimized structures of the all four orientations of DPH-β-CD following molecular mechanics simulations are depicted in Fig. 7 and the possible component binding energies and the intrinsic molecular attributes to which they will be responsive, are listed in Equations 3-8**.** Invariant factors common to mathematical description of binding energy and substituent characteristics have been ignored. Firstly, considering the lateral displacement of DPH molecule to the primary and secondary rim of β-CD, it is evident from the energy values that the β-CD-DPH_2 complex is stabilized by a binding energy of -27.264 kcal/mol as compared to -25.061 kcal/mol in case if β-CD-DPH_1. These energy optimizations were supported by the non-bonding interactions, primarily by van der Waals forces and electrostatic interactions between the drug and the cyclic oligosaccharide molecule (Eqn. 3-6). This spatial preference of secondary rim over primary rim is also depicted in Fig. 7a and 7b where a deeper inspection revealed the close proximity of the DPH to primary hydroxyl groups. The other two possible inclusion compound models formed from the interaction of one β-CD and one DPH molecule are depicted in Fig.7c and 7d. The phenyl rings of DPH were included into the cyclodextrin cavity through the primary hydroxyl groups edge (Fig. 7c) or through the secondary hydroxyl groups edge (Fig. 7d), which rendered the aliphatic chain closer to primary and secondary edges, respectively.

The DPH insertion through the narrower rim was more favourable as illustrated by the energy characteristics and molecular attributes (Eqns. 3, 4, 7, 8). As compared to parallel models, β-CD-DPH_3 and β-CD-DPH_4, demonstrated higher energy stabilities which accounted for -40.501 kcal/mol and -31.677 kcal/mol, respectively. Furthermore, unlike the parallel models, β-CD-DPH_3 and β-CD-DPH_4, demonstrated not so close energy stabilities in the form of electrostatic stability**.** However, the insertion through the secondary ring resulted in a β-CD conformation with torus distortions and may create higher steric hindrance for the penetrant (Fig. 7d). The results can also be deduced in a way that the phenyl rings are more favoured towards the secondary rim due to availability of more space. The aforementioned results suggested a possible molecular arrangement for the inclusion

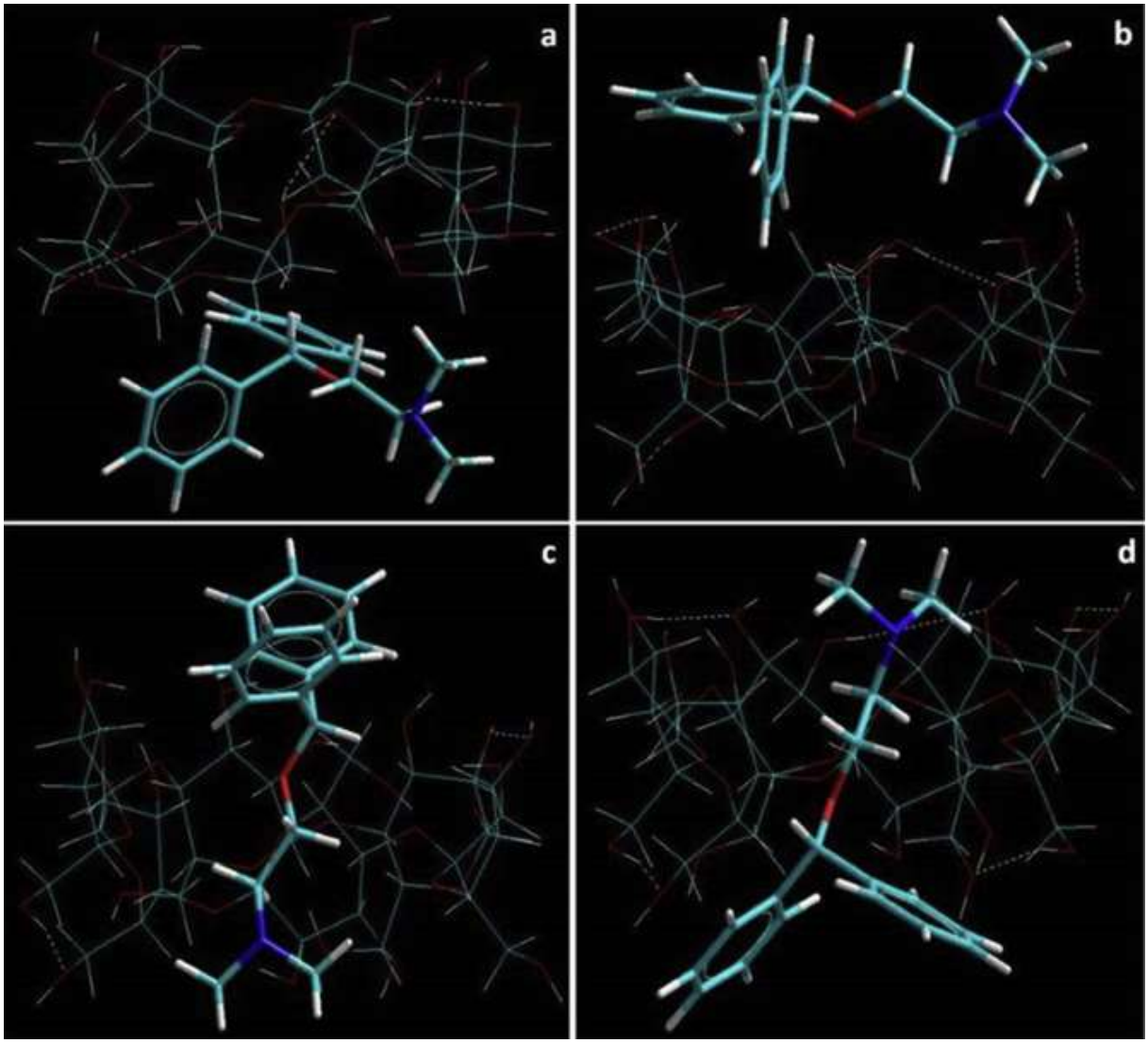

Fig. 7. Energy minimized constrained models of the drug-cyclic oligosaccharide assemblies derived from molecular mechanics calculations: (a) β-CD-DPH_1; (b) β-CD-DPH_2; (c) β-CD-DPH_3 and (d) β-CD-DPH_4. Colour codes for elements are: Carbon (cyan), Hydrogen (white-tubes), Oxygen (red) and Nitrogen (blue).

complex in a way that the drug molecule may bury itself in the cavity of the β-CD in a configuration in which half the molecule may lie in one monomer and other half may lie in the other monomer which in turn may be held in position due to the formation of close spatial interaction – clarify statement. These results further provide support to our speculation as to the use of β-CD for the taste masking of DPH as postulated earlier in the manuscript. The inclusion complex so formed between DPH and β-CD is intending to mask the taste by encasing the bitter drug inside the cyclic oligosaccharide moiety. The modelling results and the taste masking postulation in line with previous reported studies by Reddy et al. and Conway, respectively[33,34].

3.8.3 Prediction of the mucoadhesive potential of the U-D-WAF

The monomer length for the polymer chain depicting molecular structures of the polymers were determined on the basis of equivalent grid surface area covered by the polymers so that the inherent stereo-electronic factors at the interaction site can be perfectly optimized. The set of low-energy conformers that were in equilibrium with each other was identified and portrayed as lowest energy conformational model. The mucoadhesive potential of the **U-D-WAF** was elucidated as a measure of specific chemical interactions between the individual polymers (HPC and PAA) and polymeric matrix (HPC/PAA) and the glycosylated oromucopeptide analogue after geometrical optimization using energy minimizations. It is evident from Eqns. 8-10, that the formation of HPC-PAA (in vacuum) was accompanied by potential and steric energy stabilization of -43.660 kcal/mol. **Molecular modelling studies accounted for the specific interactions between polymer segments and provided an estimate for when the two polymers form a compatible blend as they have a negative free energy of mixing[34]**. This confirmed the compatibility of the polymers and stability of the **U-D-WAF** in dried state. Furthermore, the energy data displays the involvement of non bonding interactions in form of electrostatic interactions and van der Waals forces. The energy minimization seem inherent from rotation of saccharide and acrylate residues producing strain due to steric interactions which in turn are relieved by the inclusion of bond length and angle adjustment with respect to the degrees of freedom of the system. This steric adjustment may lead to the formation of H-bonds between PAA and HPC as displayed in Fig. 8a. The aliphatic groups in PAA moved along with pendent groups of HPC to their nearest minimum downhill of the starting point during minimization, driving the molecule through unfavourable regions. These large steric interactions may cause pendent groups to overcome torsional barriers presenting a larger accessible potential energy surface for interaction forming an interconnected polymeric matrix. This interconnected network

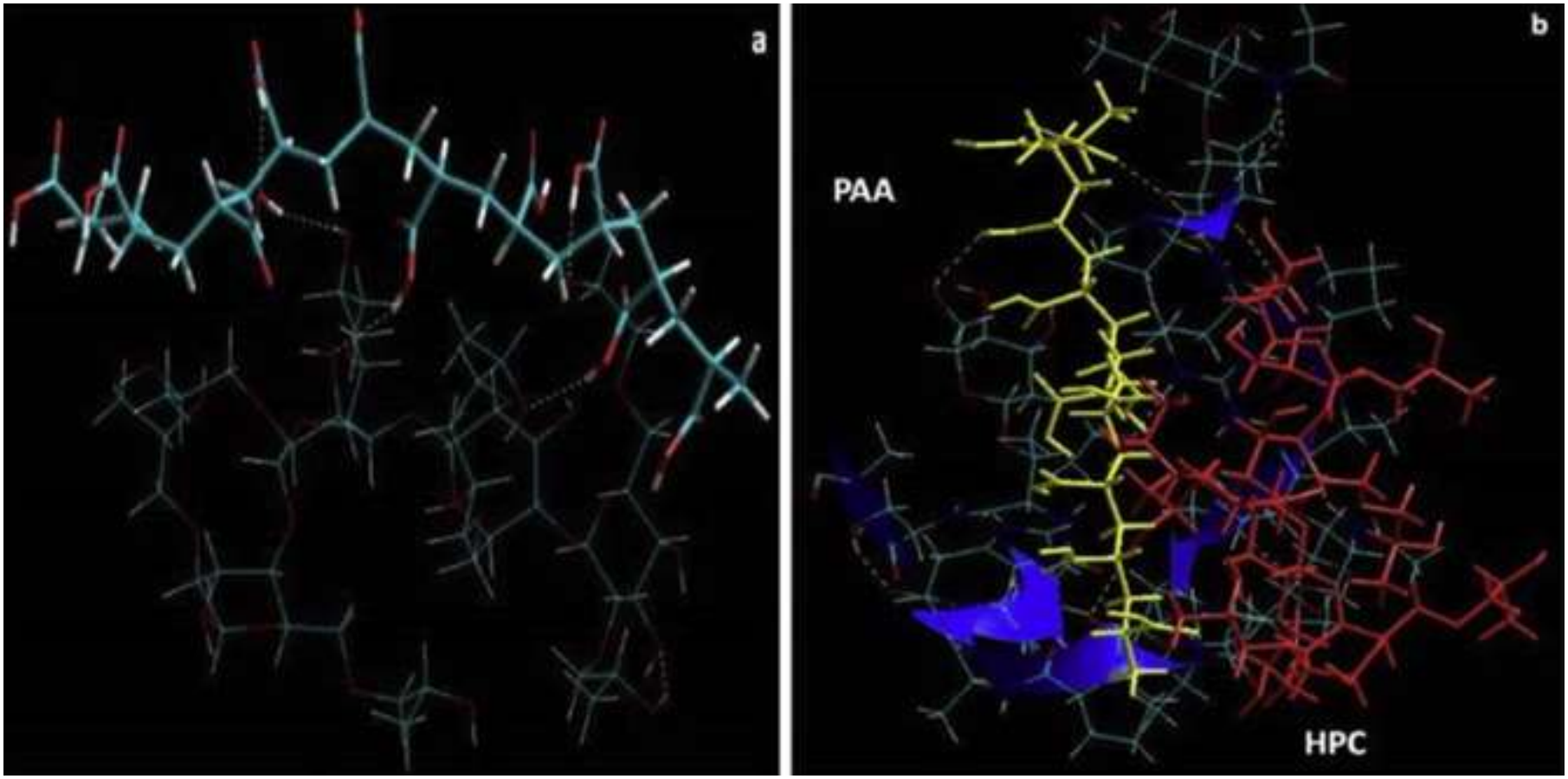

Fig. 8. Energy minimized constrained models of (a) HPC/PAA polymer matrix and (b) HPC/PAA – MUC polymer-protein complex assemblies derived from molecular mechanics calculations. Colour codes for elements are: Carbon (cyan), Hydrogen (white-tubes), Oxygen (red) and Nitrogen (blue).

structure may provide the necessary physicomechanical properties to the **U-D-WAF**. It may also be responsible for the formation of the porous structure (instead of a continuous polymer structure) which led to the rapid inflow of water in the matrix thereby disintegrating it in a very short time.

We further carried out the molecular computations to ascertain the thermodynamic/energetic changes that may occur due to interaction of the polymeric matrix with the mucosal peptide in the form of HPC/PAA-MUC (Fig. 8b, Eqns. 11-13). The energy minimizations were found to be a collective phenomenon including non-bonding interactions in the form of van der Waals forces and electrostatic interactions (Eqns. 9, 10, 11 and 12). Furthermore, the H-bonding between HPC-PAA, HPC-MUC and PAA-MUC contributed to a stress transduction requiring a large fraction of the surface to establish connectivity between chemically transformed regions (Fig. 8b). The binding energy of the polymer matrix with MUC was highly stabilized at -89.100 kcal/mol confirming the significant interactions among the polymer entities and the oromucopeptide (Fig. 8b and Eqn. 13). The H-bonds formed between the polymer matrix and the MUC further depicts the interaction profile of the polymer and the protein. A deeper inspection shows that the specificity of this complex arises due to hydrophobic interactions of the methyl groups of the mucopeptide residues with oxygen atoms of the polymers (Fig. 8b).

4. CONCLUSIONS

The use of the Box-Behnken Design proved to be an invaluable tool in assessing the influence of **U-D-WAF** matrix constituents upon drug release characteristics of a rapidly disintegrating, low density wafer intended for rapid oramucosal drug delivery. HPC concentration was seen to be a rate-limiting factor for disintegration, correspondingly impacting the drug release and permeation, over a short period of time, to a greater degree compared to either PAA or SSG. PAA demonstrated its ability to slowly release drug over a certain time period but this manipulation of drug release from matrix was demonstrated only after the matrix disintegration had occurred. This finding is critical since it implies the potential to further enhance bioavailability of the model drug as less of the drug will be swallowed as an intra-oral suspension and become lost to conventional digestive processes. *In vivo* findings revealed that the drug released from optimized **U-D-WAF** is more rapidly able to achieve a larger concentration of drug systemically than currently commercially available oral comparator products. Furthermore, the molecular mechanics studies

corroborated the possible role of β-CD towards the taste-masking action of the **U-D-WAF** and the possibility of the **U-D-WAF** to act as a mucoadhesive system. Thus, the Molecular Mechanics Computations that involved the modelling of HPC/PAA polymeric matrix with the oral mucosa suggest that **U-D-WAF** can be used as a potential mucoadhesive drug delivery device for both immediate and prolonged release purposes.

Declaration of interest

The Authors confirm that there are no conflicts of interest.

Acknowledgements

This work was funded by the National Research Foundation (NRF) and the Technology Innovation Agency (TIA) of South Africa.

Ethical approval

Animal ethics clearance for this study was obtained from the Animal Ethics Screening Committee of the University of the Witwatersrand (Ethics clearance no. 2007/56/04).

References

1. J.A. DiMasi, R.W. Hansen, H.G. Grabowski, The price of innovation: new estimates of drug development costs, J. Health Econ. 22 (2003) 151-85.
2. A-S.B. Brown, E. Hamed E, OraVescent® Technology offers greater oral transmucosal delivery, Drug Deliv. Technol. 7 (2007) 42–45.
3. S.M. Alshehri, J-B. Park, B.B. Alsulays, R.V. Tiwari, B. Almutairy, A.S. Alshetaili, J. Morotta, S. Shah, V. Kulkarni, S. Majumdar, S.T. Martin, S. Mishra, L.Wang, M.A. Repka, Mefenamic acid taste-masked oral disintegrating tablets with enhanced solubility via molecular interaction produced by hot melt extrusion technology, J. Drug Deliv. Sci. Tec. 27 (2015) 18-27.
4. D. Harris, J.R. Robinson, Drug delivery via the mucous membranes of the oral cavity, J. Pharm. Sci. 81 (1992) 1-10.
5. M. Morishita, N.A. Peppas, Is the oral route possible for peptide and protein delivery? Drug Discovery Today. 11 (2006) 905-910.
6. O. Anderson, O.K. Zweidorff, T. Hjelde, E.A. Rodland, Problems when swallowing tablets. A questionnaire study from general practice, Tidsskr Nor Laegeforen. 115 (1995) 947–949.
7. L. Dobetti, Fast-melting tablets: developments and technologies, PharmaTech Europe. 12 (2000) 32-42.

8. H. Seager, Drug-delivery products and the Zydis fast-dissolving dosage form, J. Pharm. Pharmacol. 50 (1998) 375-382.
9. S.V. Sastry, J.R. Nyashadham, J.A. Fix, Recent technological advances in oral drug delivery – a review, Pharm. Sci. Technolo. Today. 3 (2003) 138-145.
10. S. Bredenberg, M. Duberg, B. Lennernäs, H. Lennernäs, A. Pettersson, M. Westerberg, C. Nyström, *In vitro* and *in vivo* evaluation of a new sublingual tablet system for rapid oramucosal absorption using fentanyl citrate as the active substance, Eur. J. Pharm. Biopharm. 20 (2003) 327-334.
11. L. Segale, L. Maggi, E. O. Machiste, S. Conti, U. Conte, A. Grenier, C. Besse, Formulation design and development to produce orodispersible tablets by direct compression, J. Drug Deliv. Sci. Tec. 17 (2007) 199-203.
12. W. Habib, R. Khankari , J. Hontz, Fast-dissolving drug delivery systems, clinical review in therapeutics, Crit. Rev. Ther. Drug Carrier Syst. 17 (2000) 61-72.
13. R.H. Bogner, M.F. Wilkosz, Fast dissolving tablets, US Pharmacist. 27 (2002) 34-43.
14. A.K. Banga, Y.W. Chien, Systemic delivery of peptides and proteins, Int. J. Pharm. 48 (1988) 15-50.
15. R. Patel, V. Pillay, Y.E. Choonara, T. Govender, A novel cellulose based hydrophilic wafer matrix for rapid bioactive delivery, J. Bioact. and Compat. Pol. 22 (2007) 119-142.
16. K.K. Peh, C.F. Wong, Polymeric films as a vehicle for buccal delivery: swelling, mechanical and bioadhesive properties, J. Pharm. Sci. 2 (1999) 53-61.
17. S.K. El-Arini, S.D. Clas, Evaluation of disintegrating testing of different fast dissolving tablets using the texture analyser, Pharm. Dev. Technol. 7 (2002) 361-71.
18. V.S. Rudraraju, C.M. Wyandt, Rheology of microcrystalline cellulose and sodiumcarboxymethyl cellulose hydrogels using a controlled stress rheometer: part II, Int. J. Pharm. 292 (2005) 63-73.
19. Heldman DR, Lund DB. Handbook of food engineering. 2nd ed. CRC Prss Online; 2006.
20. L.I. Giannola, V. De Caro, G. Giandelia, M.G. Siragusa, G. Campisi, A. Wolff, Current status in buccal drug delivery, Pharm. Tech. Eu. 20 (2008) 32-39.
21. P. Van der Bijl, A.D. Van Eyk, I.O.C. Thompson, Effects of freezing on the permeability of human buccal and vaginal mucosa, S. Afr. J. Sci. 94 (1998) 499-502.
22. L.I. Giannola, V. De Caro, G. Giandelia, M.G. Siragusa, C. Tripodo, A.M. Florena, G. Campisi, Diffusion of nalltrexone accross reconstituted human oral epithelium and histomorphological features, Eur. J. Pharm. Biopharm. 65 (2007) 238-246.

23. J.C. Eichhorst, M.L. Etter, N. Rousseaux, D.C. Lehotay, Drugs of abuse testing by tandem mass spectrometry: A rapid, simple method to replace immunoassays, Clinical Biochemistry. 42 (2009) 1531–1542.
24. A. Kaufman, U. Jegle, A. Dreyer, R.E. Majors, Using DMSO as an injection solvent to increase sample load in preparative, Agilent Technologies. 2005
25. K. Walters-Thomson, W.D. Mason, Method for the determination of diphenylhydramine in rabbit whole blood by High-Performance Liquid Chromatography (HPLC) and ultrviolet (UV) detection in conjugation with gas chromatography (GC) with mass selective detection, Pharm. Res. 2 (1992) 929-932.
26. P. Kumar, V. Pillay, Y.E. Choonara, G. Modi, D. Naidoo, L.C. du Toit, In silico theoretical molecular modeling for Alzheimer's disease: The nicotine-curcumin paradigm in neuroprotection and neurotherapy, Int. J. Mol. Sci. 12 (2011) 694-724.
27. F. Amin, T.J. Shah, R. Dua, R. Mishra R, Superdisintegrants: an economical alternative, Pharmafocus Asia. 3 (2008) 47-48.
28. D. Kaushik, H. Dureja, T.R. Saini, Orally disintegrating tablets: An overview of melting mouth tablet technologies and techniques, Tablets, Capsules. 2 (2004) 30-36.
29. D.S. Jones, B.C.O. Muldoon, A.D Woolfson, F.D. Sanderson, An examination of the rheological and mucoadhesive properties of poly(acrylic acid) organogels designed as platforms for local drug delivery to the oral cavity, J. Pharm. Sci. 96 (2007) 2632-2646.
30. **E. Carretti, L. Dei, P. Baglioni. Aqueous polyacrylic acid based gels: physicochemical properties and applications in cultural heritage conservation, Prog. Colloid Polym. Sci. 123 (2004) 280-283.**
31. D.C. Warhurst, J.C. Craig, I.S. Adagu, D.J. Meyer, Y. Sylvia, S.Y. Lee, The relationship of physico-chemical properties and structure to the differential antiplasmodial activity of the cinchona alkaloids, Malaria J. 2 (2003) 26.
32. D.A. Pearlman, D.A. Case, J.W. Caldwell, W.S Ross, T.E. Cheatham, S. De-Bolt, D. Ferguson, G. Seibel, P. Kollman, AMBER, a package of computer programs for applying molecular mechanics, normal mode analysis, molecular dynamics and free energy calculations to simulate the structural and energetic properties of molecules, Comp. Phys. Commun. 91 (1995)1-3.
33. M.N. Reddy, T. Rehana, S. Ramakrishna, K.P.R. Chowdary, P.V. Diwan, β-Cyclodextrin Complexes of Celecoxib: Molecular-Modelling, Characterization, and Dissolution Studies, AAPS PharmSci. 6 (2004) E7.
34. B.R. Conway, Delivering scents and flavours - lessons from the pharmaceutical industry, Chem. Today. 26 (2008) 66-67.
35. A.R. Tiller, B. Gorella, Estimation of polymer compatibility from molecular mechanics calculations, Polymer. 35 (1994) 3251-3259.